

Differential Patterns of Glial Fibrillary Acidic Protein-Immunolabeling in the Brain of Adult Lizards

SAMIR ABOUCHA,¹ ABDELHADI LAALAOUI,¹ MARIANNE DIDIER-BAZES,^{2,3}
MICHELLE MONTANGE,^{2,3} HOWARD MICHAEL COOPER,^{3,4}
AND HALIMA GAMRANI^{1*}

¹Laboratoire de Neurosciences, Université Cadi Ayyad, Faculté des Sciences Semlalia, Marrakech 4000, Morocco

²Institut National de la Santé et de la Recherche Médicale, U433, Neurobiologie Expérimentale et Physiopathologie, Faculté de Médecine Laënnec, 69372 Lyon, France

³Institut Fédératif des Neurosciences de Lyon, Hôpital Neurologique, 69003 Lyon, France

⁴Institut National de la Santé et de la Recherche Médicale, U371, Cerveau et Vision, 69675 Bron, France

ABSTRACT

The present study describes by means of immunohistochemistry the comparative distribution of glial fibrillary acidic protein (GFAP)-positive cells in the forebrain and midbrain of three species of lizards: *Eumeces algeriensis*, Scincoidae; *Agama impalearis*, Agamidae; *Tarentola mauritanica*, Gekkonidae. In the species studied, the different types and proportions of glial cells expressing GFAP showed considerable variation. These cells include radial glia, oval cells, tanycytes, ependymocytes, glia limitans, and astrocytes. In *Eumeces*, astrocytes are particularly abundant and their processes form numerous perivascular end-feet; in addition well-differentiated ependymal cells and glia limitans express GFAP. These mature glial features are concordant with the relatively advanced phylogenetic level of *Eumeces*. In *Tarentola*, relatively few GFAP-expressing glial cells are observed, consisting mainly of radial glia and tanycytes. These features indicate a relatively immature state of the glial cell populations in this species. In *Agama*, GFAP-immunostained cells are confined to the periventricular and subpial brain areas; the ventricular lining contains numerous GFAP-immunopositive tanycytes and well-differentiated glia limitans. This pattern indicates that the glial cell profile in *Agama* exhibits characteristics intermediate between *Eumeces* and *Tarentola*, a feature which is discordant with the relatively primitive phylogenetic level of Agamidae compared to Gekkonidae. Together, the results of the present study provide novel data on the characterization of GFAP-expressing cell populations in different species of lizards. We suggest that the different glial patterns observed in the lizard brain correlates with developmental and functional aspects. *J. Comp. Neurol.* 464:159–171, 2003.

© 2003 Wiley-Liss, Inc.

Indexing terms: astrocytes; tanycytes; radial glia; cortex; reptiles; evolution

The glial system has evolved considerably both ontogenetically and phylogenetically in brain structures of vertebrates. Several glial and nonglial cell types expressing glial fibrillary acidic protein (GFAP) have been reported in mammalian and nonmammalian species. These cell types include radial glia, oval cells, tanycytes, ependymocytes, glia limitans, and astrocytes (Onteniente et al., 1983; Pixley and De Villis, 1984; Bodega et al., 1990; Monzon-Mayor et al., 1990a,b; Lauro et al., 1991; Bruni, 1998). Expression of GFAP in these cells is partly related to phylogeny and also reflects the state of functional maturation of various brain structures. In this context, the study of glial cell components in different species is highly

relevant to the understanding of the brain architectural organization.

Grant sponsor: French/Moroccan collaborative grant; Grant number: SVS/121/97.

*Correspondence to: Halima Gamrani, Laboratoire de Neurosciences, Université Cadi Ayyad, Faculté des Sciences Semlalia, B.P. 2390, Marrakech 40000, Morocco. E-mail: gamrani@ucam.ac.ma

Received 19 December 2000; Revised 10 February 2003; Accepted 2 April 2003

DOI 10.1002/cne.10781

Published online the week of July 28, 2003 in Wiley InterScience (www.interscience.wiley.com).

Functionally, glial cells play a crucial role in the development and homeostasis of the central nervous system (CNS). Several types of glial cells are distinguished in the brain of vertebrates. Tanycytes possess morphological and biochemical characteristics of immature radial glia. These cells, present in adult animals, give rise to radially oriented processes (Sarnat, 1992) that extend for variable distances into the adjacent neuropil, where they terminate on blood vessels, neurons, or at the brain surface (Bruni, 1998). Tanycytes express vimentin, the cytoskeletal protein expressed also by radial glia, as well as immature neurons and astrocytes (Dahl et al., 1981; Bignami et al., 1982; Houle and Federof, 1983). Tanycytes are probably implicated in neuroendocrine function (Bruni, 1998).

Astrocytes, the main cell type expressing GFAP in the brain parenchyma of mammals, display numerous processes and communicate with each other through specialized junctions. They constitute a syncytium that structurally consolidates the fully differentiated brain tissue and functionally allows coordinated responses of coupled astrocytes in brain structures (Nagy and Rash, 2000). Astrocytic processes establish several contacts, notably with blood vessels, neurons, and other glia, by which the astrocytes carry out localized regulation of neuronal activity, mainly in metabolic support (Hertz, 1992; Forsyth et al., 1996), homeostasis regulation (Walz et al., 1994), and neurotransmission (Schousboe et al., 1993). Ependymocytes and astrocytes forming the glia limitans are specialized glial cells which border the ventricles and the brain surface, respectively; they serve mainly a protective function by regulating exchanges between the cerebrospinal fluid (CSF) and the brain tissue (Bruni et al., 1985; Bruni, 1998; Saunders et al., 1999a).

Radial glia, located in the ventricular and subventricular zones, play a role of precursor cells (Soula et al., 1990), support neuronal migration during development, and provide nutritional and neurotrophic signals to other brain cells (Chanas-Sacre et al., 2000). The radial glial cells constitute a major cell type in the developing brain of

numerous nonmammalian and mammalian vertebrates. In mammals, these cells differentiate into astrocytes when neuronal migration is completed (Choi et al., 1983; Voigt, 1989; Culican et al., 1990; Tuba et al., 1997). It has also been recently hypothesized that radial glia represent the precursors of neuronal and glial cells in the developing and mature nervous system (Alvarez-Buylla et al., 2001; Götz et al., 2002). By contrast, in nonmammalian species radial glial cells persist into adulthood as a major component of glia (Onteniente et al., 1983; Monzon-Mayor et al., 1990a,b; Lauro et al., 1991; Wicht et al., 1994; Lazzari et al., 1997; Kálmán, 1998). During radial glial differentiation in mammals, transitional forms between radial glia and astrocytes are observed postnatally (Pixley and De Villis, 1984), but in nonmammalian vertebrates these forms persist in adulthood (Bodega et al., 1990; Monzon-Mayor et al., 1990a). Transitional glial cells with an oval cell body which express both GFAP and vimentin have also been reported during development in the lizard (Monzon-Mayor et al., 1990a).

Comparative studies of the glial system in different lineages of the vertebrate phylum have shown considerable variation in glial cell composition. In mammals and birds, astrocytes are predominant, whereas radial glia are found only during brain development (Sharp, 1972; Onteniente et al., 1983; Kálmán and Hajós, 1989; Voigt, 1989; Kálmán et al., 1998). Tanycytes have been described in mammals mainly during development, but in adulthood they are only found along the hypothalamic third ventricle (for review, see Bruni, 1998). In adult reptiles, tanycytes are distributed throughout the brain ependyma more widely than in mammals. In fact, in reptiles these cells have been described in the hypothalamic, lateral, and mesencephalic ventricles (Hetzl, 1977; Fernandez-Llebrez et al., 1981; Wouterlood, 1981; Lazzari and Franceschini, 2001). Astrocytes are also found in reptiles, amphibians, and teleosts, although radial structures are predominant (Onteniente et al., 1983; Monzon-Mayor et al., 1990a,b; Lauro et al., 1991; Wicht et al., 1994; Lazzari et al., 1997; Lazzari and Franceschini, 2001). In reptiles, and notably in lizards, only a few studies of the glial network have been performed, namely, in *Gallotia galloti* (Yanes et al., 1990; Monzon-Mayor et al., 1990a,b; 1998), *Lacerta lepida* (Gianonatti et al., 1987; Bodega et al., 1990) and *Podarcis sicula* (Lazzari and Franceschini, 2001).

The present comparative study is aimed at a detailed investigation of the features of glial cells in three species of lizard using GFAP as a marker. The studied species belong to three distinct families from the evolutionary point of view (Estes et al., 1988): *Agama impalearis* (Agamidae; the most primitive family), *Eumeces algeriensis* (Scincoidae; the most advanced family), and *Tarentola mauritanica* (Gekkonidae; an intermediate family). It is therefore of special interest to compare the GFAP expression patterns in these species, also in view of its potential significance in maturational, functional, and phylogenetic aspects.

MATERIALS AND METHODS

Animals

In this study we used the brains of 24 adult lizards *Agama impalearis*, *Eumeces algeriensis*, and *Tarentola*

Abbreviations

3V	third ventricle
ADVR	anterior dorsal ventricular ridge
Aq	aqueduct (fourth ventricle)
Ctx	general cortex
DC	dorsal cortex
DMC	dorsomedial cortex
dgc	dorsal geniculatum corpus
flm	fasciculus longitudinalis medialis
lfb	lateral forebrain bundle
lgc	lateral geniculatum corpus
LC	lateral cortex
IV	lateral ventricle
MC	medial cortex
Nip	interpeduncularis nucleus
nac	nucleus accumbens
nam	nucleus amygdalae
nsm	nucleus septalis medialis
OT	optic tectum
ot	optic tract
Ras	superior raphe nucleus
S	septum
sl	sulcus limitans
Sph	nucleus sphericus
St	striatum
sv	sulcus ventralis

mauritanica (n = 8 per species). The animals were captured in August in the semiarid region of the Marrakech province (Morocco) under institutional approval and authorization. The animals were housed for 1–3 weeks in boxes at room temperature under the natural dark–light cycle and fed with insects (cricket and locust). Special care was taken to avoid any discomfort or suffering of the animals.

Western blotting

Groups of animals (n = 4 per species) were decapitated and the whole brain quickly frozen. Tissue was homogenized in 0.1 M phosphate-buffered saline (PBS), pH 7.4 (150 μ l/mg of tissue wet weight) denatured in 125 mM Tris-HCl, pH 6.8, containing 10% β -mercaptoethanol, 10% SDS, 1% bromophenol blue, 10% glycerol. Proteins were separated by electrophoresis (SDS-PAGE) on 9% acrylamide-bis acrylamide gel (50 μ l of samples were loaded for GFAP analysis). They were blotted on nitrocellulose sheets (Schleicher & Schuell, Keene, NH, BA-S 85, 150 mA, 2 hours). The membranes were saturated in 0.1 M PBS, pH 7.4, containing 5% of skimmed milk and 1% Triton X100. Immunodetection of GFAP was performed by incubating the membrane in GFAP polyclonal antibodies directed against purified GFAP isolated from cow spinal cord (Dako, Copenhagen, Denmark, Z0334, Lot/ch.-B. 096 (302) diluted 1:3,000 in PBS, pH 7.4, containing 0.1% Triton X100 and 1% skimmed milk). After washing in the same buffer the membranes were incubated for 2 hours at room temperature with goat antirabbit-streptavidin immunoglobulin (1:10,000; Dako). The peroxidase activity was revealed by treating sections in 0.03% diaminobenzidine (DAB; in 0.05 M Tris buffer, pH 7.5) containing 0.01% H₂O₂. Controls of rat cortex samples were used to compare GFAP-immunoreactive bands to those of lizards.

Immunohistochemistry

Groups of animals (n = 4 per species) were anesthetized with sodium pentobarbital (40 mg/Kg i.p.), and perfused transcardially with cold saline followed by 4% paraformaldehyde in 0.1 M PB, pH 7.4. The brains were fixed in the same fixative for 12 hours at 4°C, dehydrated in graded alcohol solutions, transferred through serial dilutions of polyethylene glycol (Sigma, St. Louis, MO) and embedded in pure polyethylene glycol. Frontal sections (20 μ m) were cut with a microtome and collected in PBS. Free-floating sections were incubated in GFAP polyclonal rabbit antibodies (diluted 1:500 in PBS, pH 7.4, containing 0.1% Triton X100 and 1% bovine serum albumin). After washing in the same buffer the sections were incubated for 2 hours at room temperature with biotinylated goat antirabbit immunoglobulin (1:2,000; Dako) and thereafter in streptavidin-peroxidase (1:2,000; Dako). The peroxidase activity was revealed by treating sections with 0.03% DAB (Sigma) in 0.05M Tris buffer, pH 7.5, containing 0.01% H₂O₂. The sections were then collected, dehydrated, and mounted in Eukitt (Sigma). Photomicrographs were obtained using a Scan-Jet scanner and arranged in figures using Adobe PhotoShop 5.0.

RESULTS

GFAP detection by Western blot

The use of GFAP antibodies after immunotransfer of brain protein extracts of *Eumeces*, *Agama*, and *Tarentola*

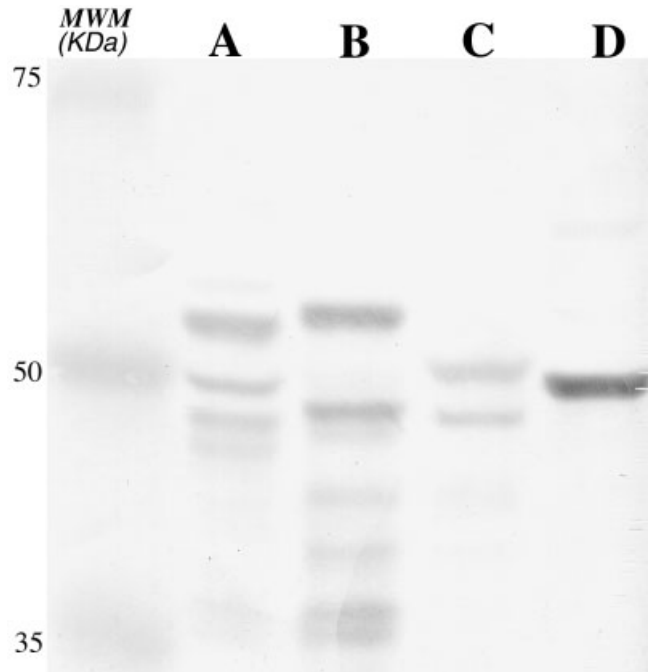


Fig. 1. Western blot of total protein samples from brain extracts of *Eumeces* (A, 20 μ g), *Agama* (B, 20 μ g), *Tarentola* (C, 30 μ g), and rat (D, 20 μ g). Note the presence of three bands (55, 51, and 48 kDa) in *Eumeces*. Two bands were detected in *Agama* (56 and 49 kDa) and *Tarentola* (52 and 48 kDa). In rat frontal cortex a unique band with 51 kDa was revealed. Note the presence of low MW discrete bands in *Agama* brain extracts, probably corresponding to degradation product of GFAP in this species. MWM, molecular weight marker.

revealed a major band with molecular weights (MWs) of 55, 56, and 52 kDa, respectively (Fig. 1). In *Eumeces* brain extracts the GFAP antibody recognized two additional immunoreactive bands with 51 and 48 kDa. Whereas in *Agama* and *Tarentola* only one additional band was revealed with, respectively, 49 and 48 kDa. In contrast to brain extracts of studied lizards, GFAP antibody recognize in rat cerebral cortex a unique band with 51 kDa.

GFAP-immunopositive cells

GFAP immunohistochemistry in the brain of the lizards revealed many positive elements, including radial glia, oval cells, tanycytes, ependymocytes, and astrocytes. The distribution of these immunostained cell populations revealed notable species differences.

The terms used to describe the different GFAP-immunostained cell types in this study are based on the distribution of the labeled cell bodies and on the morphology of cell processes. The term "radial glia" is applied to glial cells with somata located in the ventricular zone with radially oriented processes that terminate with end-feet both along the ventricular border and subpially (see also Hartfuss et al., 2001). The term "tanycytes" is used to describe ependymal cells with somata residing in the ependymal lining and a unique radial process comparable to that of radial glia, which extends for variable distances in the neuropil. The term tanycytes has been used in previous studies in lizards (Hetzler, 1977; Wouterlood, 1981; Lazzari and Franceschini, 2001). The term "radial

structures" is used to designate both radial glia and tanycytes. The ependymocytes have their somata in the ependyma, as the tanycytes, but, at variance with the latter cells, they are devoid of radial processes. In contrast, the term "astrocytes" is used to designate intraparenchymal somata with numerous processes, conferring a star-like shape to these cells. The oval cells also have intraparenchymal cell bodies and give origin to a unique radial process. The term "oval cells" has also been used in a previous investigation in lizards (Monzon-Mayor et al., 1990a).

Telencephalon

Ventricular walls. In all the examined lizards the ventricular walls of the cortex are formed mainly by tanycyte somata (*Agama*, Fig. 2A; *Eumeces*, Fig. 2B; *Tarentola*, Fig. 2C) which are immunostained by GFAP antibodies. In the ependymal layer bordering the anterior dorsal ventricular ridge (ADVR), GFAP immunostaining is usually less intense than in the adjacent cortex. However, distinct interspecific differences are observed in the ADVR. In *Agama* (Fig. 2a1), no GFAP immunoreactivity is observed in the ependymal layer. In *Eumeces* (Fig. 2b1), scattered ependymal cells devoid of GFAP-immunoreactive processes are detected. In contrast, the ADVR borders in *Tarentola* (Fig. 2c1) show mainly GFAP-positive radial processes.

The ependymal layer bordering the septum and the striatum shows GFAP immunoreactivity that also differs among species. In *Agama* the ependyma contains mainly tanycyte somata with long radial processes invading the neuropil (Figs. 3A, 4A). In *Eumeces* (Figs. 3B, 4B) GFAP-positive labeling is observed mainly in ependymal somata, whose processes are devoid of immunostaining. In *Tarentola* the ependyma bordering the striatum (Fig. 3C) shows mainly immunoreactive tanycyte somata and numerous radial glia end-feet. These radial glial processes extend towards the ventral surface of the brain (Fig. 3c). The ependyma bordering the septum (Fig. 4C) contains only a few tanycyte somata.

Cerebral cortex. In the cortex the GFAP-immunoreactive components are represented mainly by tanycyte processes in *Agama* (Fig. 2A) and *Eumeces* (Fig. 2B). Tanycyte processes extend mainly towards local blood vessels or within the cortical parenchyma. Some radial glial processes, which form subpially the glia limitans, are also observed in these two species. In *Agama* the radial processes emanating from tanycytes and radial glia are observed mainly in the medial cortex (MC), dorsomedial cortex (DMC), and dorsal cortex (DC), whereas only randomly oriented processes are observed in the lateral cortex (LC). In *Eumeces*, radial processes are observed mainly in the MC and DMC. In contrast, in the DC and LC randomly oriented processes are predominant. In cortex of *Tarentola* (Fig. 2C) the most obvious feature is represented by numerous radial glial processes that terminate subpially; a few tanycyte cells are also observed (Fig. 2c1). Radial processes are observed in both the MC and DMC, whereas randomly oriented processes are detected in the DC and LC.

Astrocyte somata are observed in the cortex of all lizard species examined and they are relatively dense in *Agama* (Fig. 2a2) and *Eumeces* (Fig. 2b2), but sparser in *Tarentola* (not shown). In *Eumeces*, immunoreactive processes, emanating from either astrocytes and/or radial processes,

surround the blood vessels throughout the entire cortex (Fig. 2B).

Glia limitans. In *Agama* (Fig. 3A) a dense layer of immunoreactive processes is observed in the subpial matter. These processes emanate from GFAP-positive astrocytes (Fig. 3A). In *Eumeces* (Fig. 3B), dense immunoreactivity is also observed in the subpial matter. In the ventral limiting membrane of *Tarentola*, weak GFAP immunoreactivity is observed. Obvious GFAP-positive processes and/or end-feet, emanating either from radial processes (Fig. 3C) or astrocytes (Fig. 3F), are present.

Septum and striatum. In *Agama* the striatum (Fig. 3A) shows straight tanycyte processes that spread radially into a zone intermediate between the periventricular and subpial regions. These processes mainly terminate near the local blood vessels. Astrocyte somata are located in the dorsal part of the striatum and in the nucleus accumbens (Fig. 3A). Astrocyte somata are also observed within the lateral forebrain bundle (Fig. 3A) and in the amygdala (Fig. 3D). In *Agama*, tanycyte processes also invade the septum (Fig. 4A) throughout its extent. Astrocytes are present mainly in the septal nucleus impar (not shown) and are less frequently observed in the medial septal nuclei (Fig. 4A).

In the striatum (Fig. 3B) and septum (Fig. 4B) of *Eumeces*, fine GFAP-positive processes, emanating mainly from small astrocytes, are observed in the amygdala (Fig. 3E), as well as in all the other telencephalic structures. These processes form numerous perivascular end-feet (Fig. 4B).

The *Tarentola* striatum (Fig. 3C) contains tanycyte and radial glial processes that end either on blood vessels or subpially. In the septum of this species (Fig. 4C), many randomly oriented processes but few radial processes are present. Astrocyte somata are not found in these structures, although numerous astrocytes are observed in the amygdala (Fig. 3F).

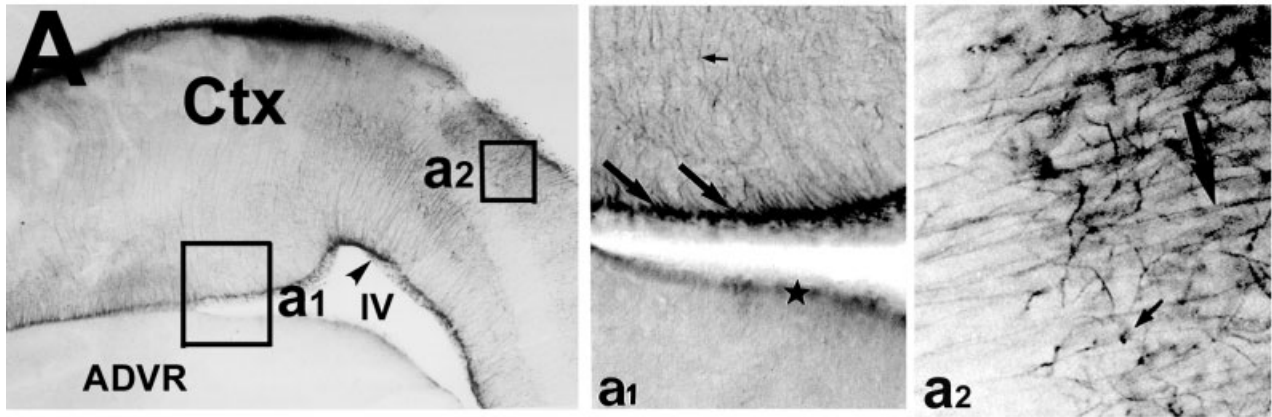
Nucleus sphericus. Dense GFAP-immunoreactive protoplasmic astrocytes are concentrated within the parenchyma of the nucleus sphericus in *Agama* (Fig. 4D), whereas radial processes are not observed. In *Eumeces* only a few small astrocyte somata with thin processes, radial processes, or perivascular end-feet, are seen in the nucleus sphericus (Fig. 4E). In *Tarentola* (Fig. 4F) mainly radial processes, perivascular end-feet, and a few astrocytes are observed in this structure.

Diencephalon

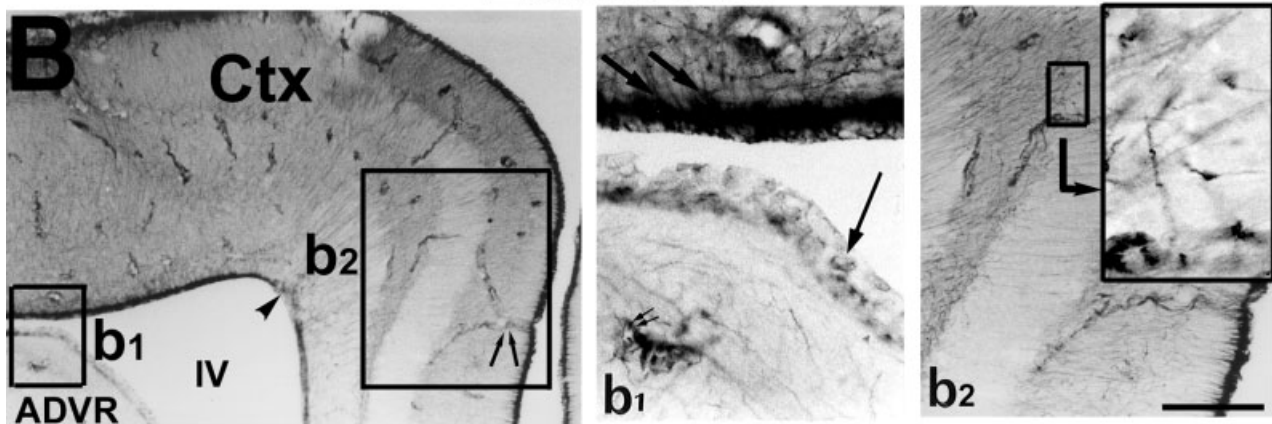
Ventricular walls. In *Agama* the ependyma lining the third ventricle shows an intense immunostaining that labels numerous positive tanycyte somata at both the thalamic (Fig. 5A) and hypothalamic (Fig. 5A,D) borders. In *Eumeces* the ependyma bordering the thalamus shows mainly GFAP-positive ependymocytes (Fig. 5B) devoid of processes. In the hypothalamus of this species GFAP-immunoreactive tanycyte somata are also observed in the ependyma (Fig. 5E). In *Tarentola* (Fig. 5C) GFAP immunoreactivity stains tanycyte somata at the thalamic (Fig. 5C) and hypothalamic (Fig. 5F) borders. Intense immunopositive perivascular end-feet are observed in the diencephalon of this species (Fig. 5C).

Visual structures. In *Agama*, visual structures show coarse and intensely immunoreactive processes that contrast with the more slender processes in the adjacent neuropil. GFAP-positive astrocytes are observed in the

Agama



Eumeces



Tarentola

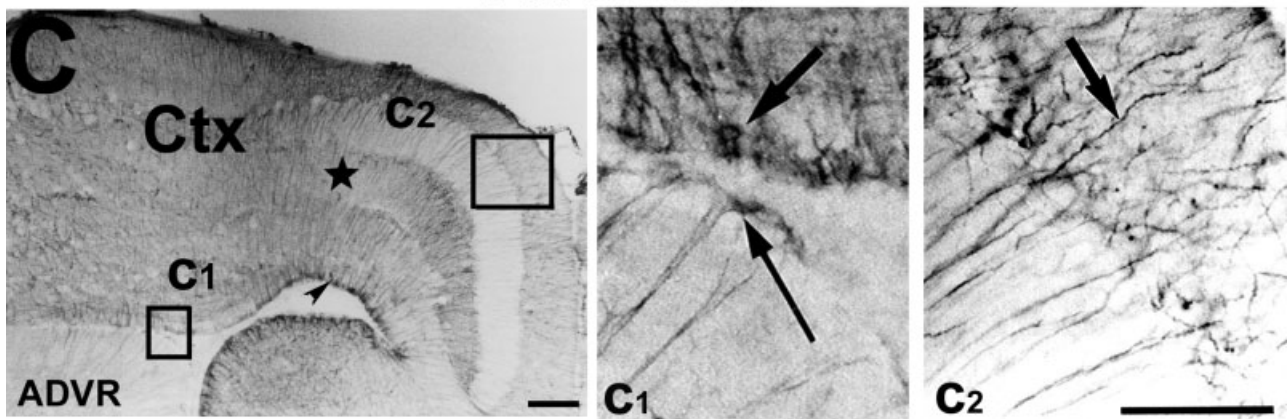
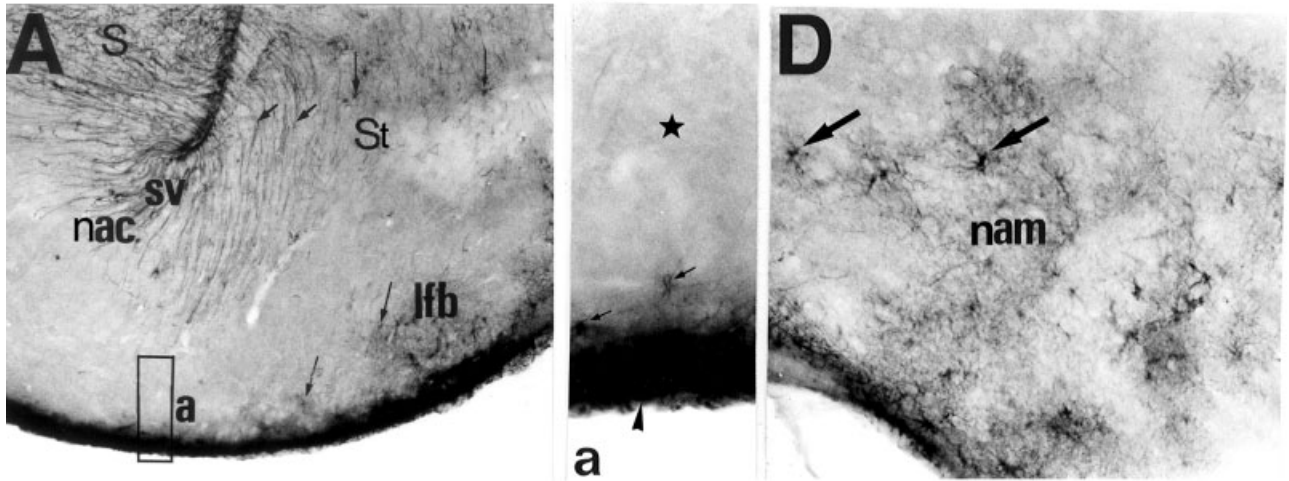


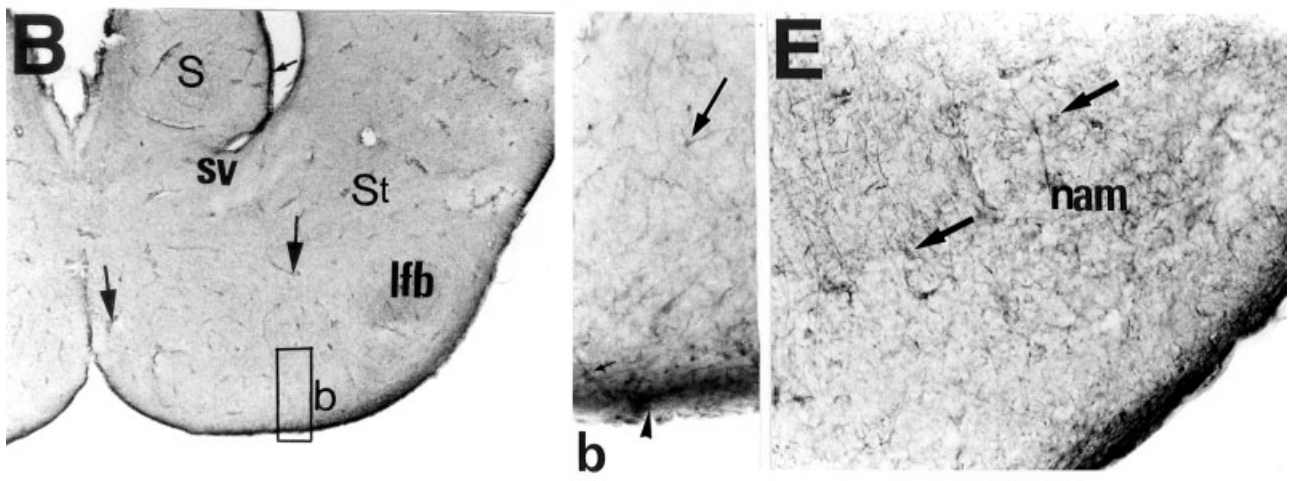
Fig. 2. Peroxidase immunohistochemistry with GFAP antibody in dorsal telencephalon of *Agama* (A), *Eumeces* (B), and *Tarentola* (C) in the cortex (Ctx) and the anterior dorsoventral ridge (ADVR). A: In *Agama* cortex, note the presence of GFAP-positive tanycytes with long processes (arrowhead). Perivascular end-feet are not observed. The ADVR is essentially devoid of immunolabeling. **a1**: High magnification of the ependymal layer bordering the ADVR showing weak immunoreactivity (star). In the cortex, note the presence of tanycyte somata (large arrows) and radial processes (small arrow). **a2**: High magnification of the medial cortex showing astrocyte somata (small arrow) and radial processes (large arrow) forming subpial end-feet. B: In the cortex of *Eumeces*, immunostaining is observed in tanycyte somata (arrowhead). Note the presence of immunolabeling around blood vessels (double arrows). **b1**: High magnification of the ependymal layer bordering the cortex showed tanycyte somata (large ar-

rows). The ependyma bordering the ADVR shows some immunoreactive ependymocytes (thin arrow). Small double arrows point to perivascular end-feet. **b2**: High magnification of the pial region showing less immunoreactive radial processes. Note the presence of perivascular end-feet (double arrows). Note in the insert small immunoreactive astrocyte somata (small arrows). IV, lateral ventricle. C: In *Tarentola* cortex, numerous radial glial processes (star) are observed, these radial fibers give origin to glial end-feet. Tanycytes are also observed (arrowhead). **c1**: High magnification showing tanycyte cell (large arrow). In the ADVR, GFAP-positive radial fibers give origin to glial processes that reach the ventricular border (thin arrow). **c2**: High magnification of the medial cortex showing GFAP radial glial processes of the subpial end-feet (arrows). Scale bars = 100 μ m in C (applies to A–C), 50 μ m in C2 (applies to a1–b1, c1, c2), 100 μ m in b2.

Agama



Eumeces



Tarentola

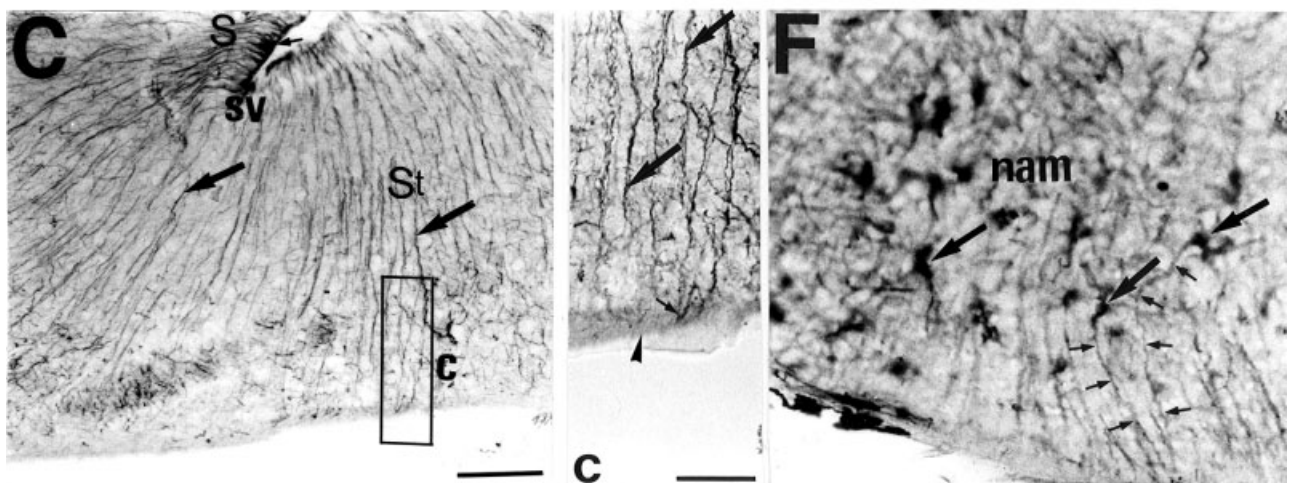


Figure 3

optic chiasm (not shown), optic tract (Fig. 5a), and corpus geniculatum dorsalis and lateralis (Fig. 5A).

In *Eumeces*, thin GFAP-positive processes and astrocyte somata are seen in the optic chiasm (not shown) and optic tract (Fig. 5b).

In the visual structures of *Tarentola*, peculiar helicoidal-shaped GFAP-positive processes are seen within the optic tract. These processes are thick and bulbous (Fig. 5c) and are not observed in other structures or in the other species studied. A few astrocyte somata are present in the optic chiasm (not shown).

Thalamus. In *Agama*, immunolabeling is restricted to the thalamic periventricular and lateral areas (Fig. 5A). Tanycyte processes exhibit a limited length and do not extend farther than the periventricular zone. Astrocyte somata are observed in the lateral forebrain bundle (Fig. 5a), in the habenular nuclei, and in the periventricular region (Fig. 5G).

In *Eumeces*, thin, stained processes, emanating from small GFAP-positive astrocytes, are observed in all thalamic regions. These processes form numerous small perivascular end-feet throughout the thalamus. Astrocytes are also observed in the habenular nuclei of this species (Fig. 5H).

In *Tarentola* (Fig. 5C), dense radial processes, emanating from either tanycytes or radial glia, are more extensive and form large perivascular end-feet. Astrocyte somata are essentially observed in the habenular nuclei (Fig. 5I).

Hypothalamus. In *Agama* (Fig. 5A,D), immunolabeling is intense in the hypothalamic region. Tanycyte processes extend throughout this structure. A few GFAP-positive astrocyte somata are observed.

In *Eumeces* (Fig. 5B,E), thin, GFAP-positive processes, emanating from either small astrocytes or tanycytes (Fig. 5E), are observed in the hypothalamus. These processes form several perivascular end-feet. Small astrocyte somata are scattered throughout the hypothalamus.

Fig. 3. GFAP localization in the telencephalon of *Agama* (A,D), *Eumeces* (B,E), and *Tarentola* (C,F) at the level of the striatum (St; A–C) and the amygdala nucleus (nam; D–F). A: Ependymal layer of the sulcus ventralis (sv) of *Agama* displaying tanycytes with straight processes. These cells spread radially in the intermediate zone of the striatum (small arrows) but do not reach the surface of the brain. Astrocytes (long arrows) are detected in the striatum (St), the lateral forebrain bundle (lfb), and throughout the subpial area. a: High magnification of the glia limitans showing a dense GFAP immunolabeling (arrowhead) with astrocyte cells (small arrows) subpially. The deeper region is devoid of immunolabeling (star). S = septum. B: The ependymal layer of *Eumeces* shows mainly GFAP-positive ependymocytes (small arrow) in septum. Note the presence of perivascular labeling in all structures (large arrows) b: High magnification of the ventral area showing a moderate GFAP labeling in the glia limitans (arrowhead). Note the presence of astrocyte cells subpially (small arrow), and others dispersed in the brain tissue (long arrow). C: Photomicrograph showing GFAP-positive tanycyte somata (small arrow) and radial glial processes projecting subpially (large arrows) in *Tarentola*. c: High magnification of the ventral area shows weak GFAP immunoreactivity (arrowhead). Immunolabeling is detected in GFAP-positive radial processes (large arrows). Few processes end in the external limiting membrane (small arrow). D: Photomicrograph showing astrocyte cells (large arrows) in the amygdalae of *Agama*. E: Dispersed astrocyte cells (large arrows) are observed in the amygdalae of *Eumeces*. F: Large astrocytes (large arrows) are detected in *Tarentola* displaying processes that sometimes end subpially (small arrows). Scale bars = 250 μ m for A–C (in C), 60 μ m for a–f (in c).

In *Tarentola* the hypothalamus (Fig. 5C,F) shows less immunoreactivity than that observed in the thalamic region. Radial processes, emanating from tanycyte somata, terminate occasionally in perivascular end-feet (Fig. 5F). Astrocyte somata are rarely observed.

Mesencephalon

Ventricular walls. In the aqueduct, GFAP-positive tanycytes with radial processes and ependymocytes devoid of processes are observed in *Agama* (Fig. 6A). In *Eumeces* (Fig. 6B), ventricular borders contain mainly GFAP-positive ependymocytes and a few tanycytes, whereas in *Tarentola* (Fig. 6C) the ventricular walls show mainly GFAP-positive tanycyte somata.

In the ependyma bordering the optic tectum GFAP-positive tanycyte somata and/or radial glia end-feet are observed in all the studied lizards (Fig. 6G–I).

Tegmentum. The *Agama* tegmentum shows dense and localized astrocyte cells in several mesencephalic regions: the fasciculus longitudinalis medialis, raphe nuclei, the nucleus interpeduncularis, and throughout the peripheral region of the mesencephalon (Fig. 6A). Another GFAP-positive element observed in the *Agama* mesencephalon is represented by oval cells (Fig. 6D), characterized by oval or round-shaped cell bodies, a unique cell process, and a general close proximity to blood vessels (Fig. 6d).

In *Eumeces* (Fig. 6B), thin, GFAP-positive processes, emanating from small immunoreactive astrocyte somata, are observed throughout the mesencephalon. Numerous perivascular end-feet are also observed throughout the parenchyma. No oval cells are observed.

Numerous tanycyte processes are observed in *Tarentola*. Astrocyte somata are less obvious compared to the other lizards (Fig. 6C,F). GFAP-positive oval cells are also observed (Fig. 6f).

Optic tectum. The *Agama* optic tectum (Fig. 6G) shows immunoreactive radial processes, emanating from either radial glia or tanycytes. Intensely stained protoplasmic astrocytes are also detected (Fig. 6G). In *Eumeces* (Fig. 6H), thin GFAP-positive radial processes, small astrocyte somata, and perivascular end-feet are observed. In *Tarentola* (Fig. 6I) a dense network of regularly oriented radial processes is evident, whereas astrocyte somata are rarely observed.

DISCUSSION

GFAP labeling specificity and overall pattern of distribution

The antibodies against GFAP used in our study resulted in immunopositive labeling in all lizards. In Western blot these antibodies recognize in *Eumeces*, *Agama*, and *Tarentola* a major immunoreactive protein of 55, 56, and 52 kDa, respectively, contrasting with the single 51 kDa immunoreactive band in rat. Similar observations of higher MW have been reported in turtle (Dahl, 1976) and in goldfish (Dahl et al., 1985). Dahl (1976) described in brains of several species, including teleosts, amphibians, and birds, the presence of GFAP protein homologous to that detected in mammals, which migrates as a single band of 54 kDa. Among studied species, differences in MW of the major GFAP-immunoreactive band could be ascribed either to interspecific differences in molecular com-

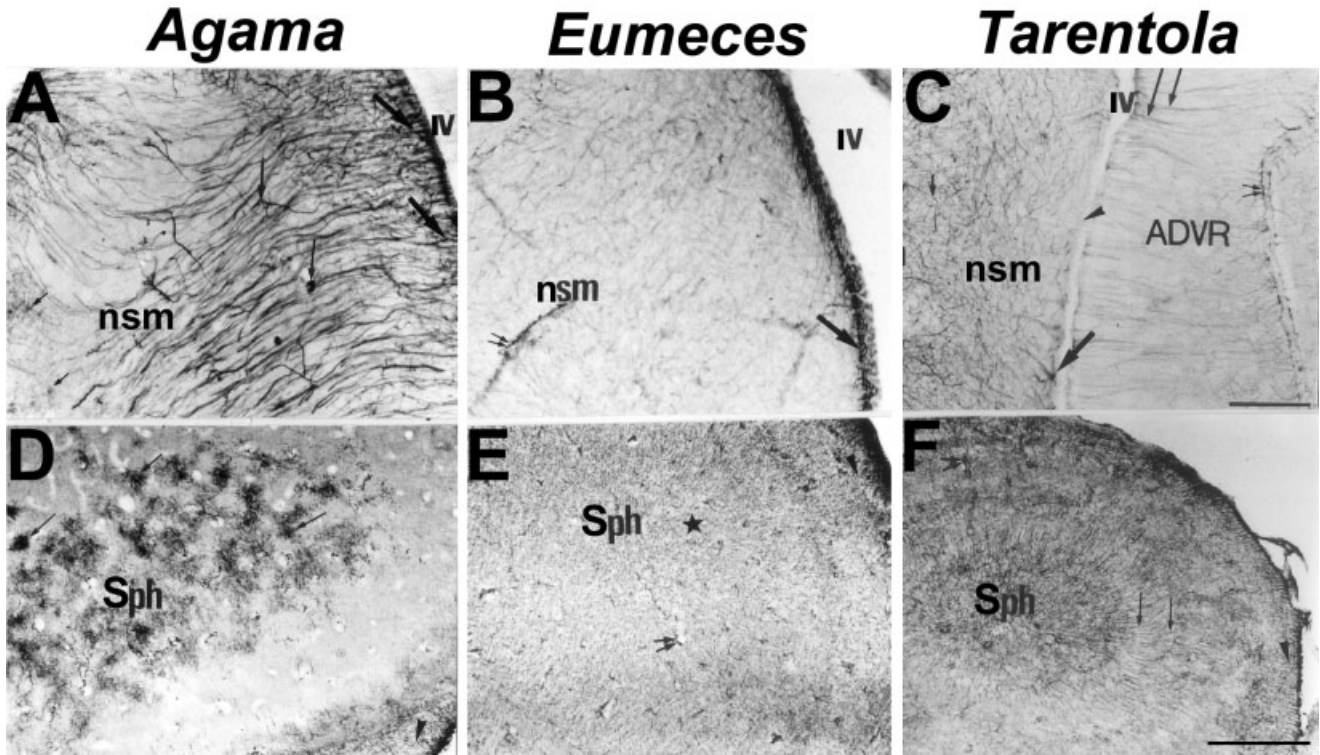


Fig. 4. Immunohistochemical detection of GFAP in *Agama* (A,D), *Eumeces* (B,E), and *Tarentola* (C,F) at the level of the nucleus septalis medialis (nsm; A–C) and the nucleus sphericus (Sph; D–F). A: Photomicrograph showing tanyocyte somata (large arrows) with processes spreading radially in the septum of *Agama*. These processes terminate either in the parenchyma or the blood vessels (medium-sized arrows). Note the presence of astrocytes (small arrows) in the nucleus septalis medialis (nsm) and lateral ventricle (IV). B: The ependymal layer of *Eumeces* shows mainly ependymocytes (large arrow). Note the presence of perivascular end-feet (double arrows). C: Photomicrograph showing weak GFAP-immunoreactivity bordering the septum of *Tarentola* (arrowhead). Few tanyocyte somata (large arrow) are GFAP-positive. Inside the septum, several radial and randomly oriented processes (small arrow) are detected. Note the presence of

GFAP-positive radial processes in the anterior dorsoventricular ridge (ADVR; long arrows) and perivascular end-feet (double arrow). D: Numerous protoplasmic astrocyte somata are detected in *Agama* sphericus nuclei (arrows). Perivascular end-feet are absent in the majority of blood vessels. Few and weakly immunoreactive radial processes are revealed subpially (arrowhead). Note the absence of radial processes inside the nucleus. E: Photomicrograph showing numerous fine processes of dispersed small astrocyte somata throughout the entire nucleus of *Eumeces* (star) contacting the majority of blood vessels (double arrows). Radial processes are also observed subpially and inside the nucleus (arrowhead). F: In *Tarentola*, numerous radial processes inside the nucleus sphericus (arrows) terminating subpially (arrowhead) and perivascular end-feet (double arrows) are observed. Scale bars = 200 μm for A–C (in C), 450 μm for D–F (in F).

Fig. 5. Immunoreactivity with anti-GFAP in diencephalic structures of *Agama* (A,D,G), *Eumeces* (B,E,H), and *Tarentola* (C,F,I). A: Photomicrograph showing tanyocytes throughout the ependyma of the third ventricle in *Agama* (arrowhead) diencephalon. Processes are limited to the periventricular area (arrows) in the thalamus (Th). In the hypothalamus (Ht), processes (long arrow) reach the pia matter. The deep diencephalic area is devoid of immunoreactivity (star). Note the presence of numerous astrocyte cells in the optic tract (ot), dorsal geniculate corpus (dgc) and lateral geniculate corpus (lgc) (small arrows). a: High magnification showing coarse and intensely immunoreactive fibers in the optic tract. In this latter structure, note the presence of numerous astrocytes (large arrow). Protoplasmic astrocytes are observed in the lateral forebrain bundle (lfb) (small arrows). 3V, third ventricle. B: Photomicrograph showing immunoreactive ependymocytes of *Eumeces* in the majority of thalamic and hypothalamic ependymal borders of the third ventricle (arrowheads). Tanyocytes were observed in the ventral hypothalamic ependyma. Note the presence of perivascular end-feet throughout the whole diencephalon (arrows). Scattered astrocytes were observed throughout the whole brain parenchyma of *Eumeces*. b: High magnification of the optic tract showing astrocyte somata (large arrows). C: The ependy-

mal layer of *Tarentola* shows many tanyocyte somata throughout the whole diencephalon (arrowheads). Note the presence of large perivascular end-feet (double arrows). Astrocyte cells are not detected in visual diencephalic structures. c: High magnification of the optic tract showing thick and helicoidal GFAP-positive processes (arrows). Scale bars = 500 μm for A–C (in C); 150 μm for a–c (in c). D: Photomicrograph showing at the level of the hypothalamic ventricular border dense immunoreactive tanyocyte somata in the *Agama* (arrowheads), these cells give origin to radial processes in the periventricular area (white stars). In some regions immunoreactive ependymocyte soma devoid of GFAP-positive processes are observed (arrow). Note the presence of perivascular end-feet in the periventricular area (double arrows). 3V, third ventricle. E: Note the presence of tanyocyte somata and processes in *Eumeces* (arrowheads). F: Tanyocyte somata in *Tarentola* (arrowheads). Tanyocyte processes sometimes project to local blood vessels (small arrows). Scale bar = 150 μm for D–F (in F). G: Numerous astrocyte somata are detected in the habenular nuclei (Hab) of *Agama* (small arrows). 3V, third ventricle. H: Photomicrograph showing astrocyte somata in *Eumeces* habenula (small arrows). I: In *Tarentola*, astrocyte cells are observed in the habenula (small arrows). Scale bar = 130 μm for G–I (in I).

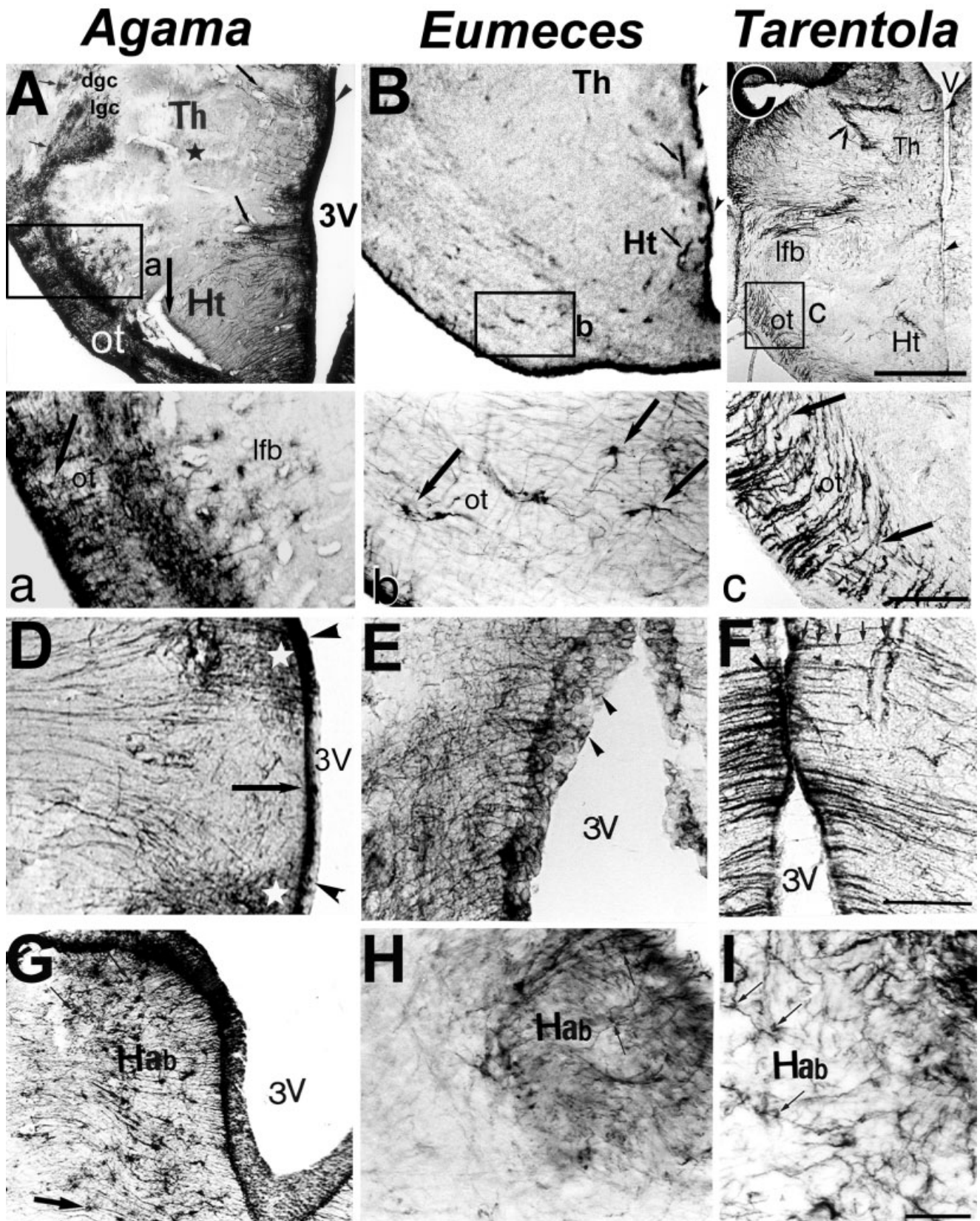


Figure 5

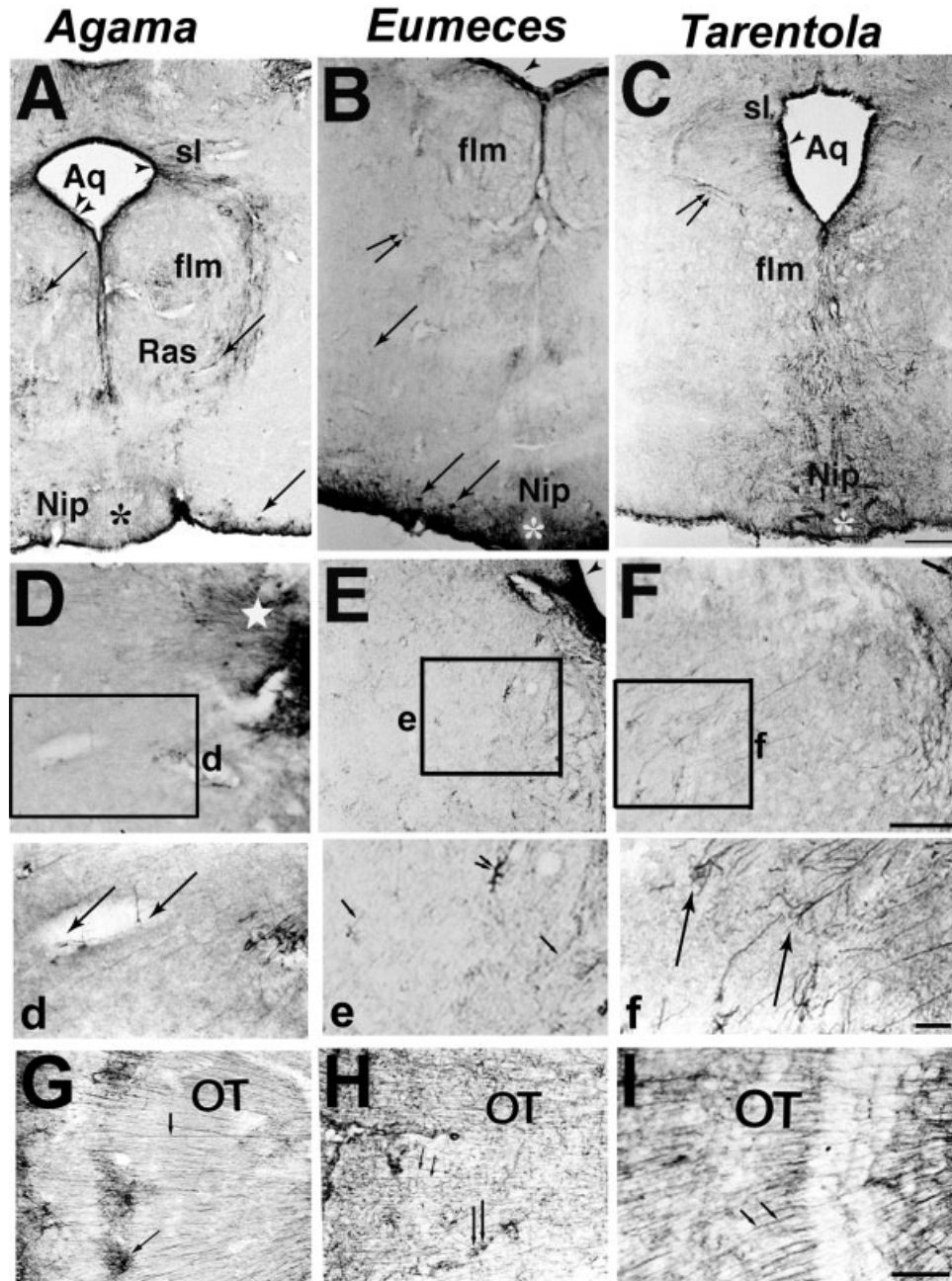


Fig. 6. GFAP localization in the mesencephalon of *Agama* (A,D,G), *Eumeces* (B,E,H), and *Tarentola* (C,F,I). A: In *Agama*, tanyocyte somata are present in the ependyma of the aqueduct (Aq; arrowhead) essentially in the sulcus limitans (sl). Ependymocytes, devoid of GFAP-positive processes, are also observed (double arrowhead). Radial processes are detected in the interpeduncularis nucleus (Nip; black asterisk). Note the presence of astrocytes in the fasciculus longitudinalis medialis (flm), superior raphe nucleus (Ras) and the ventral subpial area (arrows). B: Ependymocytes are mainly observed in the ependyma of the aqueduct of *Eumeces* (arrowhead). Tanyocyte somata are not detected. Few radial processes are observed in the interpeduncularis nucleus (white asterisk). Numerous and scattered astrocyte somata are observed throughout the whole mesencephalic parenchyma and aggregated and intensely GFAP-immunoreactive astrocytes are visualized in the ventral zone (arrows). Perivascular end-feet are distributed in the whole mesencephalon (double arrows). C: Tanyocyte somata are visualized in the ependyma of the aqueduct in *Tarentola* (arrowhead). Tanyocyte processes project mainly to local blood vessels (double arrow). Radial processes are detected in the

interpeduncularis nucleus (white asterisk). Scale bar = 300 μm for A–C (in C). D: Note the presence of tanyocyte processes (white star) in *Agama*. **d**: High magnification show GFAP-positive oval cells (arrows) with a single process in contact with local blood vessels. E: Photomicrograph showing ependymocytes in *Eumeces* ventricular borders (arrowhead). Numerous fine astrocyte processes are dispersed in the mesencephalic parenchyma. **e**: High magnification shows thin GFAP-positive processes (arrow) emanating from small astrocytes. Note the presence of perivascular end-feet (double arrows). F: In *Tarentola*, numerous tanyocyte somata are observed in the ependyma (arrow). Astrocyte somata are less frequent. **f**: High magnification shows GFAP-positive oval cells with a single process (arrows). Scale bars = 250 μm for D–F (in F), 80 μm for d–f (in f). G: Photomicrograph showing radial processes (small arrow) and protoplasmic astrocyte somata (long arrow) in *Agama* optic tectum. H: Radial processes (small arrows) and astrocyte somata (long arrows) in the optic tectum of *Eumeces*. I: Radial processes (small arrows) in the optic tectum of *Tarentola*. Scale bar = 200 μm for G–I (in I).

position or in phosphorylation state of the protein. Intraspecifically, lower MW bands could be either the consequence of proteolytic degradation or regional differences of GFAP protein expression similar to those reported in the sea bass (Dahl et al., 1985). The GFAP antibody used in our study recognizes in Western blot major proteins that have a MW ranging between 56 and 52 kDa, which is similar to that detected in other vertebrates, 54 kDa (Dahl, 1976), and in rat, 51 kDa (present study). Furthermore, immunohistochemistry showed an immunopositive reaction in all the studied lizards, confirming that GFAP is conserved through the vertebrate phyla.

The glial components in the brain of the lizards studied show differences in composition, abundance, and distribution. For example, no GFAP-immunopositive oval cells have been found in *Eumeces*, at variance with *Agama* and *Tarentola*. These latter species exhibited abundant radial glial structures (radial glia and tanycytes), whereas in *Eumeces* numerous fine GFAP-positive fibers are seen to emanate from astrocyte somata but a few radial fibers are observed. In some brain structures a peculiar distribution of GFAP-immunopositive elements is observed, especially the selective labeling of protoplasmic astrocytes in the nucleus sphericus of *Agama* and the helicoidal-shaped processes in the optic tract of *Tarentola*. These interspecific differences could reflect variations at the developmental, functional, and phylogenetic levels.

Differences in glia distribution and developmental correlates

The glial components of the brain of lizards show regional differences in the parenchymal tissue, ventricular borders, and glia limitans.

In the parenchyma, the proportion of astrocyte and radial processes differs between lizards. In *Eumeces*, astrocyte processes are widely distributed throughout nearly all brain structures. In *Agama* the proportion of astrocytes and radial processes emanating from tanycytes appears similar. In *Tarentola*, radial processes, emanating either from tanycytes and/or radial glia, are predominant. The radial glia, which typically appear during early developmental stages, express mainly vimentin as major component of the intermediate filament of immature glia (Pixley and De Vellis, 1984; Yanes et al., 1990). In adult lizards, a few vimentin-positive glial elements are present and are mainly located in the ependyma and limiting membrane, but are absent in the brain parenchyma (unpubl. obs.). During development, transition of glia phenotypic expression occurs, with a decrease in vimentin and an increase in GFAP expression (Pixley and De Vellis, 1984; Monzon-Mayor et al., 1990a; Yanes et al., 1990), and this would explain the weak vimentin immunoreactivity in adult lizards.

The *Eumeces* ependyma shows well-differentiated GFAP-positive ependymocytes devoid of radial processes. A similar GFAP-positive labeling is present in adult vertebrates (Kálmán and Hajós, 1989; Hajós and Kálmán, 1989). In *Agama* the ependyma is formed essentially by tanycytes, whereas in *Tarentola* this structure contains tanycytes and radial glia, both of which characterize early ontogenetic stages (Bruni, 1998).

Dense GFAP-positive processes and astrocytes are detected in the glia limitans of *Agama* and *Eumeces*. This distribution is similar to that observed in adult verte-

brates (Kálmán and Hajós, 1989; Hajós and Kálmán, 1989). In contrast, in *Tarentola* the glia limitans are devoid of astrocytes and only display GFAP-positive endfeet.

The widespread distribution of astrocytes throughout the brain of the adult *Eumeces*, and the well-differentiated ependyma and glia limitans in this species, suggests a relatively advanced state of glial differentiation compared to *Agama* and *Tarentola*, in which undifferentiated glial elements are also found in the adult brain.

Glial differences and functional correlates

The glial system plays an important role in the maintenance of the blood-brain barrier (Saunders et al., 1999a,b). The predominance of tanycytes in *Agama* and *Tarentola*, which establish contacts with both the CSF and the brain tissue, indicates the occurrence of indirect blood-brain exchange via the CSF, since tanycytes are reported to be involved in neuroendocrine/transport functions (Flament-Durand and Brion, 1985; Bruni et al., 1985; Sarnat, 1992; Ma, 1993). Direct blood-brain exchange could occur in *Eumeces*, via the wide distribution of astrocyte perivascular endfeet, and in *Tarentola* and *Agama* via oval cells located in close proximity to blood vessels. In addition, the high density of contacts between glial elements in the ependyma and glia limitans in *Eumeces* and *Agama* could favor the efficiency of the blood-brain barrier in both the ventricular and peripheral brain interfaces with the CSF, possibly through specialized junctions (Nakazawa and Ishikawa, 1998; Saunders et al., 1999a).

The glial differentiation has always been associated with the process of neuronal migration (Hatten, 1999). On the other hand, several studies have reported that neurogenesis can continue in the CNS of adult fish, frogs, reptiles, birds, and mammals (Pérez-Sánchez et al., 1989; Cameron et al., 1993; Goldmann, 2001). The persistence of immature radial structures in various brain regions of adult *Agama* and *Tarentola* may indicate a high degree of postnatal neurogenesis. In contrast, the wide distribution of mature astrocytes throughout most brain structures in *Eumeces* could be related to a state of reduced neurogenesis.

Agama, in particular, shows a dense distribution of astrocytes in all visual structures (optic chiasm, optic tract, optic tectum, and corpus geniculatum). The state of maturation of the glial and neural systems in these structures, in addition to the role of astrocytes in metabolism and neurotransmission (Schousboe et al., 1993; Forsyth et al., 1996), may be related to the highly developed visual behaviors (rapid locomotion and hunting behavior) required in this species.

Our findings indicate that the relative state of glial differentiation, from radial glia to astrocytes, correlates both with the neural sophistication of the system as well as with the cessation of neurogenesis. That is, structures in which neurogenesis is complete tend to have more astrocytes, while structures undergoing continuing neurogenesis retain radial glia.

Phylogenetic correlates

Reptiles represent the first vertebrate group in which astrocytes constitute a distinct cell component in the brain (Onteniente et al., 1983; Gianonatti et al., 1987; Monzon-Mayor et al., 1990a). On the other hand, mature astro-

TABLE 1. Semiquantitative Evaluation of the Distribution of GFAP-Positive Cells in Different Regions of the Lizard Brain

Brain regions	GFAP cell type	<i>Tarentola</i>	<i>Agama</i>	<i>Eumeces</i>
Telencephalon	Radial glia	+++	+	+
	Tanycytes	++	++	+
	Ependymocytes	-	+	+++
	Astrocytes	+	++	+++
	Glia limitans	-	++	++
	Perivascular end-feet	++	+	+++
Diencephalon	Radial glia	+++	+	-
	Tanycytes	+++	+++	+
	Oval cells	+	+	-
	Ependymocytes	-	+	+++
	Astrocytes	+	++	+++
	Glia limitans	-	++	++
Mesencephalon	Perivascular end-feet	++	+	+++
	Radial glia	++	+	-
	Tanycytes	++	++	+
	Oval cells	++	++	-
	Ependymocytes	-	+	++
	Astrocytes	+	++	+++
	Glia limitans	-	++	++
	Perivascular end-feet	++	+	+++

The dashed lines separate immature glial cells above from mature glial structures below. Note the predominance of immature glial cells (radial glia, tanycytes, and oval cells) in *Tarentola*, compared to the predominance of mature astrocytes in *Agama* and in particular in *Eumeces*. Symbols: - = no immunoreactive cells; +, sparse, ++, frequently observed, and +++ densely distributed immunoreactive cells.

cytes are a characteristic feature of the cortex of mammals (Kálmán and Hajós, 1989).

The present study describes the presence of astrocytes in the telencephalon of all lizards studied. In contrast, astrocytes have not been observed in the telencephalon of teleosts and amphibians, in which radial glia persist in adulthood (Onteniente et al., 1983; Lauro et al., 1991; Wicht et al., 1994; Lazzari et al., 1997). Concerning the presence of astrocytes in the telencephalon, a considerable variation is reported within and between different reptilian lineages. For example, astrocytes have been described in the snake hippocampus (a primitive cortex; Onteniente et al., 1983), in the telencephalon of the crocodilian *Caiman crocodilus* (Kálmán and Pritz, 2001), and astrocyte processes were observed in the lizard *Gallotia galloti* (Yanes et al., 1990), whereas astrocytes were not detected in the telencephalon of the lacertidae *Podarcis sicula* (Lazzari and Franceschini, 2001) or turtles (Onteniente et al., 1983; Kálmán et al., 1994).

The persistence of radial structures in adults is considered a primitive feature, observed in teleosts, in amphibians, and in certain reptiles (Onteniente et al., 1983; Monzon-Mayor et al., 1990a,b; Lauro et al., 1991; Wicht et al., 1994; Lazzari et al., 1997; Kálmán, 1998). On the other hand, in adult birds and mammals radial structures were only observed in relatively few brain regions (Onteniente et al., 1983; Kálmán and Hajós, 1989; Hajós and Kálmán, 1989; Kálmán et al., 1998). Similar data on the distribution of radial glia have been reported in the vertebrate spinal cord (Bodega et al., 1994).

In the present investigation, the distribution of radial structures (radial glia and tanycytes) showed a general inverse relation with the phylogenetic level. Thus, radial glia are frequently observed in *Tarentola* and *Agama*, but rarely seen in *Eumeces* (Table 1). In this latter species (*Eumeces*; Scincoidae), the ubiquitous distribution of astrocytes contrasts with a higher selectivity of distribution in the other lizards. In addition, the presence in *Eumeces* of well-differentiated mature ependymocytes, glia limitans, and perivascular end-feet is similar to descriptions

in mammals (Kálmán and Hajós, 1989; Hajós and Kálmán, 1989), in support of the relatively advanced phylogenetic level of this species. In *Tarentola* (Gekkonidae), the astrocytes are less frequent and GFAP-positive cells are mainly represented by undifferentiated glial elements such as radial glia, tanycytes, and oval cells (Table 1). However, *Agama*, which is considered the most primitive species, displays a GFAP-positive glial cell profile with characteristics intermediate between those of *Eumeces* and *Tarentola*, a feature which is discordant with its phylogenetic level.

CONCLUDING REMARKS

Our study shows a differential pattern of GFAP-immunopositive glial cells in three species of lizards. These differences include glial cell composition, abundance, and distribution. The different glial patterns are correlated with degrees of developmental differentiation and/or distinct roles of the glia in the maintenance of the blood-brain barrier and neurogenesis. Finally, in terms of GFAP glial architecture, we suggest that, although the Agamidae are considered the most primitive of the investigated lizards, they probably represent a state intermediate between Scincoidae and Gekkonidae.

ACKNOWLEDGMENT

The authors thank Prof. Marina Bentivoglio for help and criticism during the article revision.

LITERATURE CITED

- Alvarez-Buylla A, Garcia-Verdugo JM, Tramontin AD. 2001. A unified hypothesis on the lineage of neural stem cells. *Nat Rev Neurosci* 2:287-293.
- Bignami A, Raju T, Dahl D. 1982. Localization of vimentin, the nonspecific intermediate filament protein in embryonic glia and in early differentiating neurons. In-vivo and in-vitro immunofluorescence study of the rat embryo with vimentin and neurofilament antisera. *Dev Biol* 91: 286-295.
- Bodega G, Suarez I, Rubio M, Fernandez B. 1990. Distribution and characteristics of the different astroglial cell types in the adult lizard (*Lacerta lepida*) spinal cord. *Anat Embryol* 181:567-575.
- Bodega G, Suarez I, Rubio M, Fernandez B. 1994. Ependyma: phylogenetic evolution of glial fibrillary acidic protein (GFAP) and vimentin expression in vertebrate spinal cord. *Histochemistry* 102:113-122.
- Bruni JE. 1998. Ependymal development, proliferation and functions: a review. *Microsc Res Tech* 41:2-13.
- Bruni JE, Del Bigio MR, Clattenburg RE. 1985. Ependyma: normal and pathological: a review of the literature. *Brain Res* 9:1-19.
- Cameron HA, Wooley CS, McEwen BS, Gould E. 1993. Differentiation of newly born neurons and glia in the dentate gyrus of the adult rat. *Neuroscience* 56:337-344.
- Chanas-Sacre G, Rogister B, Moonen G, LePrince P. 2000. Radial glia phenotype: origin, regulation, and transdifferentiation. *J Neurosci Res* 61:357-363.
- Choi BH, Kim RC, Lapham LW. 1983. Do radial glia give rise to both astroglial and oligodendroglial cells?. *Dev Brain Res* 8:119-130.
- Culican SM, Baumrind NL, Yamamoto M, Pearlman AL. 1990. Cortical radial glia: identification in tissue culture and evidence for their transformation to astrocytes. *J Neurosci* 10:684-692.
- Dahl D. 1976. Isolation and initial characterization of glial fibrillary acidic protein from chicken, turtle, frog and fish central nervous systems. *Biochem Biophys Acta* 446:41-50.
- Dahl D, Rueger DC, Bignami A, Weber K, Osborn M. 1981. Vimentin, the 75,000 Dalton component of fibroblast filaments, is the major cytoskeletal component in immature glia. *Eur J Cell Biol* 24:191-196.
- Dahl D, Crosby CJ, Sethi JS, Bignami A. 1985. Glial fibrillary acidic (GFA)

- protein in vertebrates: Immunofluorescence and immunoblotting study with monoclonal and polyclonal antibodies. *J Comp Neurol* 239:75–88.
- Estes RK, Querioz DE, Gauthier DJ. 1988. Phylogenetic relationship within squamata. In: Estes R, Pergal G, editors. *Phylogenetic relationship of the lizards families*. Stanford, CA: Stanford University Press. p 119–281.
- Fernandez-Llebrez P, Becerra J, Marin-Giron F. 1981. Histological study of the ependyma of the hypothalamic third ventricle in the water snake *Natrix maura* (L). *Z Mikrosk Anat Forsch* 95:22–32.
- Flament-Durand J, Brion JP. 1985. Tancytes: morphology and functions: a review. *Int Rev Cytol* 96:121–155.
- Forsyth R, Fray A, Boutelle M, Fillenz M, Middleditch C, Burchell A. 1996. A role of astrocytes in glucose delivery to neurons. *Dev Neurosci* 18: 360–370.
- Gianonatti C, Bodega G, Gianonatti M. 1987. Glioarchitectonics of the cerebellum of the lizard (*Lacerta lepida* Daudin). Ultrastructural study. *J Hirnforsch* 28:701–705.
- Goldmann SA. 2001. Adult neurogenesis: from canaris to clinic. *J Neurobiol* 36:267–286.
- Götz M, Hartfuss E, Malatesta P. 2002. Radial glial cells as neuronal precursors: a new perspective on the correlation of morphology and lineage restriction in the developing cerebral cortex of mice. *Brain Res Bull* 57:777–788.
- Hajós F, Kálmán M. 1989. Distribution of glial fibrillary acidic protein (GFAP)-immunoreactive astrocytes in the rat brain. *Exp Brain Res* 78:164–173.
- Hatten EH. 1999. Central nervous system neuronal migration. *Annu Rev Neurosci* 22:511–539.
- Hertz L. 1992. Autonomic control of neuronal-astrocytic interactions regulating metabolic activities and ion fluxes in the central nervous system. *Brain Res Bull* 29:303–313.
- Hetzl W. 1977. The ependyma of the lateral ventricle in *Acanthodactylus pardalis* (Reptilia, Lacertidae). *Acta Anat* 97:68–80.
- Houle J, Federoff S. 1983. Temporal relationship between the appearance of vimentin and neuronal tube development. *Brain Res* 9:189–195.
- Kálmán M. 1998. Astroglial architecture of the carp (*Cyprinus carpio*) brain as revealed by immunohistochemical staining against glial fibrillary acidic protein (GFAP). *Anat Embryol* 198:409–433.
- Kálmán M, Hajós F. 1989. Distribution of glial fibrillary acid protein (GFAP)-immunoreactive astrocytes in the rat brain. I. Forebrain. *Exp Brain Res* 78:147–163.
- Kálmán M, Pritz MB. 2001. Glial fibrillary acidic protein-immunopositive structures in the brain of a crocodilian, *Caiman crocodilus*, and its bearing on the evolution of astroglia. *J Comp Neurol* 431:460–480.
- Kálmán M, Kiss A, Majorossy K. 1994. Distribution of Glial fibrillary acidic protein-immunopositive structures in the brain of the red-eared freshwater turtle (*Pseudemys scripta*). *Anat Embryol* 189:421–434.
- Kálmán M, Martin-Partido G, Hidalgo-Sanchez M, Majorossy K. 1997. Distribution of glial fibrillary acidic protein-immunopositive structures in the developing brain of the turtle (*Mauremys leprosa*). *Anat Embryol* 196:47–65.
- Kálmán M, Szekely AD, Csillag A. 1998. Distribution of glial fibrillary acidic protein and vimentin-immunopositive elements in the developing chicken brain from hatching to adulthood. *Anat Embryol* 198:213–235.
- Lauro GM, Fonti R, Margotta V. 1991. Phylogenetic evolution of intermediate filament associated proteins in ependymocytes of several adult poikilotherm vertebrates. *J Hirnforsch* 32:157–261.
- Lazzari M, Franceschini V. 2001. Glial fibrillary acid protein and vimentin immunoreactivity of astroglial cells in the central nervous system of adult *Podarcis sicula* (Squamata, Lacertida). *J Anat* 198:67–95.
- Lazzari M, Franceschini V, Ciani F. 1997. Glial fibrillary acid protein and vimentin in radial glia of *Amblystoma mexicanus* and *Triturus cristatus*: an immunocytochemical study. *J Hirnforsch* 38:187–194.
- Ma PM. 1993. Tancytes in the sunfish brain: NADPH-diaphorase histochemistry and regional distribution. *J Comp Neurol* 336:77–95.
- Monzon-Mayor M, Yanes C, Ghandour MS, De Barry J, Gombos G. 1990a. Glial fibrillary acidic protein and vimentin immunohistochemistry in developing and adult midbrain of the lizard *Gallotia galloti*. *J Comp Neurol* 295:569–579.
- Monzon-Mayor M, Yanes C, Tholey G, De Barry J, Gombos G. 1990b. Immunohistochemical localization of glutamine synthetase in mesencephalon and telencephalon of the lizard *Gallotia galloti*. *Glia* 3:81–97.
- Monzon-Mayor M, Yanes C, De Barry J, Capdevilla-Carbonell C, Renaupiqueras J, Tholey G, Gombos G. 1998. Heterogeneous immunoreactivity of glial cells in the mesencephalon of a lizard: a double labeling immunohistochemical study. *J Morphol* 235:109–119.
- Nagy JA, Rash JE. 2000. Connexins and gap junctions of astrocytes and oligodendrocytes in the CNS. *Br Res Rev* 32:29–44.
- Nakazawa E, Ishikawa H. 1998. Ultrastructural observations of astrocyte end-feet in the rat central nervous system. *J Neurocytol* 27:431–440.
- Onteniente B, Kimura H, Maeda T. 1983. Comparative study of the glial fibrillary acid protein in vertebrates by PAP immunohistochemistry. *J Comp Neurol* 215:427–436.
- Pérez-Sánchez F, Molowny A, Garcia-Verdugo JM, López-Gracia C. 1989. Postnatal neurogenesis in the nucleus sphericus of the lizard, *Podarcis hispanica*. *Neurosci Lett* 106:71–75.
- Pixley SKR, De Vellis J. 1984. Transition between immature radial glia and mature astrocytes studied with a monoclonal antibody to vimentin. *Dev Brain Res* 15:201–209.
- Sarnat HB. 1992. Role of human fetal ependyma. *Pediatr Neurol* 8:163–178.
- Saunders NR, Habgood MD, Dziegielewska KM. 1999a. Barrier mechanisms in the brain. I. Adult brain. *Clin Exp Pharmacol Physiol* 26:11–19.
- Saunders NR, Habgood MD, Dziegielewska KM. 1999b. Barrier mechanisms in the brain. II. Immature brain. *Clin Exp Pharmacol Physiol* 26:85–91.
- Schousboe A, Westergaard N, Hertz L. 1993. Neuronal-astrocytic interactions in glutamate metabolism. *Biochem Soc Trans* 21:49–53.
- Sharp PJ. 1972. Tancyte vascular patterns in the basal hypothalamus of Coturnix quail with reference to their possible neuroendocrine significance. *Z Zellforsch* 127:552–569.
- Soula C, Sagot Y, Cochard P, Dupart AM. 1990. Astroglial differentiation from neuroepithelial precursor cells of amphibian embryos: an in-vivo and in vitro analysis. *Int J Dev Biol* 34:351–364.
- Tuba A, Kallai L, Kálmán M. 1997. A rapid replacement of vimentin-containing radial glia by glial fibrillary acidic protein-containing astrocytes in transplanted telencephalon. *J Neural Transplant Plast* 6:21–29.
- Voigt T. 1989. Development of glial cells in the cerebral wall of ferrets: direct tracing of their transformation from radial glia into astrocytes. *J Comp Neurol* 289:74–88.
- Walz W, Gimpl G, Ohlemeyer C, Kettenmann H. 1994. Extracellular ATP-induced currents in astrocytes: involvement of a cation channel. *J Neurosci Res* 38:12–18.
- Wicht H, Derouiche A, Korf HW. 1994. An immunocytochemical investigation of glial morphology in the pacific hagfish: radial and astrocyte-like glia have the same phylogenetic age. *J Neurocytol* 23:565–576.
- Wouterlood FG. 1981. The structure of the mediadorsal cerebral cortex in lizard *Agama agama*: a Golgi study. *J Comp Neurol* 196:443–458.
- Yanes C, Monzon-Mayor M, Ghandour MS, De Barry J, Gombos G. 1990. Radial glia and astrocytes in developing and adult telencephalon of the lizard *Gallotia galloti* as revealed by immunohistochemistry with anti-GFAP and anti-vimentin antibodies. *J Comp Neurol* 295:559–568.